Inhibition of medulloblastoma tumorigenesis by the antiproliferative and pro-differentiative gene PC3

Stefano Farioli-Vecchioli,*,[1] Mirella Tanori,†,[1] Laura Micheli,* Mariateresa Mancuso,†
Luca Leonardi,* Anna Saran,† Maria Teresa Ciotti,* Elisabetta Ferretti,‡
Alberto Gulino,‡ Simonetta Pazzaglia,† and Felice Tirone*,[2]

*Institute of Neurobiology and Molecular Medicine, Consiglio Nazionale Ricerche, Fondazione S. Lucia, Rome, Italy; †Biotechnology Unit, ENEA CR-Casaccia, Rome, Italy; and ‡Department of Experimental Medicine and Pathology, University La Sapienza, Rome, Italy

ABSTRACT   Medulloblastoma, the most common brain tumor in childhood, appears to originate from cerebellar granule cell precursors (GCPs), located in the external granular layer (EGL) of the cerebellum. The antiproliferative gene *PC3* (*Tis21/BTG2*) promotes cerebellar neurogenesis by inducing GCPs to shift from proliferation to differentiation. To assess whether *PC3* can prevent the neoplastic transformation of GCPs and medulloblastoma development, we crossed transgenic mice conditionally expressing *PC3* (Tg*PC3*) in GCPs with *Patched1* heterozygous mice (*Ptc*$^{+/-}$), a model of medulloblastoma pathogenesis characterized by hyperactivation of the *Sonic Hedgehog* pathway. Perinatal up-regulation of *PC3* in *Ptc*$^{+/-}$/Tg*PC3* mice results in a decrease of medulloblastoma incidence of ~40% and in a marked reduction of preneoplastic abnormalities, such as hyperplastic EGL areas and lesions. Moreover, overexpression of *cyclin D1*, hyperproliferation, and defective differentiation—observed in *Ptc*$^{+/-}$ GCPs—are restored to normality in *Ptc*$^{+/-}$/Tg*PC3* mice. The *PC3*-mediated inhibition of *cyclin D1* expression correlates with recruitment of *PC3* to the *cyclin D1* promoter, accompanied by histone deacetylation. Remarkably, down-regulation of *PC3* is observed in preneoplastic lesions, as well as in human and murine medulloblastomas. As a whole, this indicates that *PC3* may prevent medulloblastoma development by controlling cell cycle and promoting differentiation of GCPs.—Farioli-Vecchioli, S., Tanori, M., Micheli, L., Mancuso, M., Leonardi, L., Saran, A., Ciotti, M. T., Ferretti, E., Gulino, A., Pazzaglia, S., Tirone, F. Inhibition of medulloblastoma tumorigenesis by the antiproliferative and pro-differentiative gene PC3. *FASEB J*. 21, 000–000 (2007)

Key Words: tumor suppressor gene · neurogenesis · cyclin D1 · Math1

Granule neurons, the most abundant neuronal cell of cerebellum, develop from committed granule cell precursors (GCPs) originating from a germinative epithelium at the roofplate of the fourth ventricle (1). GCPs migrate over the surface of the developing cerebellum to form the external granular layer (EGL), where they continue to proliferate perinatally. A failure in the control of proliferation of cerebellar precursors is thought to give rise to medulloblastoma, the most common brain tumor in childhood (2).

Sonic hedgehog (*Shh*) plays a major role in the development of the cerebellum by potently stimulating the proliferation of GCPs in the EGL (3–5). The crucial role of *Shh* in GCP proliferation is exerted through *N-Myc* and *cyclin D1*, which are among the genes most induced by *Shh* (6–10).

Components of the *Shh* pathway are frequently altered in medulloblastoma, being mutated or overexpressed. Inherited mutations in the *Patched1* gene—encoding the *Shh* receptor, which inhibits the *Shh* pathway in the absence of the ligand—lead to the development of Gorlin's syndrome, characterized by skeletal defects and predisposition to basal cell carcinomas, rhabdomyosarcoma, and a significant incidence of medulloblastoma (11). Moreover, the inactivation of *Patched1* by deletion or mutation characterizes 10–25% of sporadic medulloblastomas, suggesting that *Patched1* functions as a tumor suppressor (12–14). The subset of medulloblastomas with overactivation of the *Shh* pathway display induction of the *Shh* downstream targets *Gli1* and *N-Myc*, along with induction of markers of GCPs (15, 16). Thus, medulloblastomas characterized by a deregulation of the *Shh/Patched* pathway very likely originate from GCPs.

A key contribution to the understanding of the molecular mechanisms of medulloblastoma tumorigenesis comes from mouse models [for review, see (2)]. Inactivation of one *Patched1* allele leads to the development of spontaneous medulloblastomas, which confirms the key role of the *Shh* pathway in the etiology of the tumor (17, 18). *Patched1* heterozygous mice survive to adulthood, but 8–30% develop medulloblastoma after 2–6 months of age, and more than 50% present ectopic EGL regions, indicative of a preneoplastic

---

condition (17, 19, 20). The frequency of ectopic EGL and of medulloblastoma is dramatically increased by radiation exposure of *Patched1* heterozygous mice immediately after birth, when EGL precursors are actively proliferating (21, 22).

We have recently observed that the *PC3* gene plays a role in the control of GCP differentiation. *PC3*, which we originally isolated as a gene induced at the onset of the neuronal differentiation elicited by nerve growth factor (23), possesses antiproliferative properties and is expressed in a restricted number of tissues and in neuronal precursors undergoing a neurogenic asymmetric division (23–27). During neurogenesis, *PC3* accelerates the shift of neural precursors from proliferation to differentiation, thereby promoting the generation of new neurons (28). The marked action exerted by *PC3* in GCPs is dual: delay of G_1 phase progression through inhibition of *cyclin D1* and induction of *Math1* (28), a gene required for maturation and differentiation of GCPs (29). We proposed that these actions of *PC3* synergize to effect in GCPs terminal cell cycle exit and differentiation.

Here, we tested the hypothesis that the antiproliferative/prodifferentiative effects of PC3 in GCPs may counteract the development of medulloblastoma in *Patched1* heterozygous mice. In parallel, we investigated the physiological implication of PC3 in murine and human medulloblastoma.

MATERIALS AND METHODS

Mouse lines and genotyping

A bitransgenic mouse line was used, carrying two transgenes: βACT-tTA transgene, encoding the tetracycline-regulated TransActivator driven by the human β-actin promoter (βACT), and TRE-*PC3* transgene, carrying the *PC3* coding region under control of the tetracycline responsive elements (TRE). The single transgenic mouse lines were generated as described (28), exploiting the tet-off system to control the activation of the *PC3* transgene (30), and were maintained in a BDF1 (C57BL/6 × DBA/2) background. In bitransgenic mice the βACT promoter drives the transcription of the tTA TransActivator (the second transgene), which in turn activates TRE-*PC3* by binding the upstream TREs. Doxycycline inactivates tTA, consequently repressing the expression of TRE-*PC3*.

Mice lacking one *Patched1* allele, generated through disruption of exons 6 and 7 in 129/SV ES cells and maintained in a CD1 background (18), were crossed for this study to the binary transgenic βACT-tTA/TRE-*PC3*. The mouse lines and the F1 progeny resulting from crossings were genotyped using primers specific to the tTA and to the TRE regions for βACT-tTA/TRE-*PC3* mice and to the neo insert and wt regions for heterozygous *Patched1* knockout mice, as described (28, 18).

Animal treatment and irradiation

Animals were housed under conventional conditions with a 12 h light–dark schedule. Embryonic day 1 (E1) was considered completed at midnight of the day after mating. Brains collected from postnatal day 14 (P14) mice were fixed and stored as described (28). Doxycycline hydrochloride (150 μg/ml; MP Biomedicals, Eschwege, Germany) was supplied to mice in the drinking water supplemented with 5% sucrose, from the day of mating to day 14 of pregnancy, after which it was removed. This allowed the expression of transgenic *PC3* after about E18, given the time necessary to metabolize doxycycline.

Mice were irradiated at P1 with with an X-ray dose of 3 Gy using a Gilardoni CHF 320 G X-ray generator (Gilardoni S.p.A., Mandello del Lario, Italy) operated at 250 kVp, 15 mA, with filters of 2.0 mm Al and 0.5 mm Cu (HVL=1.6 mm Cu).

Tumor quantification and histological analysis

Mice were observed daily for their whole life span. On decline of health (*i.e.*, severe weight loss, paralysis, ruffling of fur, or inactivity), they were sacrificed and autopsied. Brains were fixed in 4% buffered formalin. Samples were then embedded in paraffin wax according to standard techniques, sectioned serially and stained with hematoxylin/eosin.

Immunohistochemistry, antibodies, BrdU labeling, and TUNEL analysis

Immunohistochemistry was performed on serial sections with 10 μm thickness of brains from P14 mice using mouse monoclonal antibodies raised against *cyclin D1* (Santa Cruz Biotechnology, Santa Cruz, CA, USA; clone 72–13G, 1:75), *NeuN* (Chemicon International, Temecula, CA, USA; MAB377; 1:100) and phospho-histone H2A.X (Upstate Biotechnology, Lake Placid, NY, USA; clone JBW301; 1:100), or using rabbit polyclonals that recognize *cyclin D2* (Santa Cruz, SC-181; 1:100), *cyclin B1* (Santa Cruz, SC-752; 1:200), *NeuroD1* (R&D Systems, Minneapolis, MN, USA; AF2746; 1:100), and *PC3* (A3H, 1:50) (24). Antiphospho-histone H2A.X marks DNA repair foci, being histone H2A.X rapidly phosphorylated following DNA double-strand breaks. A3H antibody recognizes both the transgenic PC3 and the endogenous mouse PC3 (*i.e., Tis21*) proteins. Binding of primary antibodies was revealed using FITC-conjugated goat anti-mouse or TRITC-conjugated goat anti-rabbit secondary antibodies (Jackson ImmunoResearch, West Grove, PA, USA; 1:100 and 1:200, respectively).

Analysis of BrdU incorporation in the EGL was performed using P14 mice injected with BrdU (90 mg/kg, i.p.) 1.5 h before sacrifice. This period of incorporation was judged appropriate to label mainly S phase cells, based on the duration of the S and G_2/M phases in GCPs of mice at this age (31). Sections were permeabilized and stained with mouse monoclonal anti-BrdU (Amersham Biosciences, Arlington Heights, IL, USA) as described (28).

Cells positive for BrdU incorporation or for expression of other markers were calculated as percent ratio of the number of labeled cells to the total number of cells (visualized by counterstaining nuclei with Hoechst 33258 (1 μg/ml in PBS, Sigma, St. Louis, MO, USA), for the entire length of the EGL in each photomicrograph field. Nuclei with condensed and fragmented chromatin were considered apoptotic and were not counted.

Apoptotis was measured on sections by TUNEL (terminal deoxynucleotidyl transferase-mediated dUTP-conjugated nick end labeling) (32) using the *in situ* cell death detection kit (Roche Products, Hertfordshire, UK), followed by staining with 0.5% DAB, according to the manufacturer's instruction. Apoptotic nuclei were quantified as percent ratio of the total number of cells in the EGL, visualized by hematoxylin/eosin staining.

Images of the immunostained sections were obtained with

an BX51 microscope (Olympus, Tokyo, Japan) connected to a Diagnostic Instruments camera 1.3.0 (Sterling Heights, MI, USA), or by laser scanning confocal microscopy using a CLSM 510 microscope (Zeiss, Jena, Germany). Measurements of positive cells were performed by the I.A.S. software (Delta Systems, Rome, Italy).

In situ hybridization

Preparation of sections and hybridization were performed as previously reported, with some modifications (28). Hybridization was performed with digoxigenin labeled specific antisense probes (Transcription kit; Roche). Samples were incubated overnight at 4°C with alkaline phosphatase-conjugated antidigoxigenin antibody (Roche; 1:2000), washed and processed for colometric detection using nitroblue-tetrazolium/5-bromo-4-chloro-3-indolyl-phosphate (NTB/BCIP).

Specific antisense riboprobes were synthesized for: *a) Math1*, by T7 polymerase from mouse *Math1* cDNA (vector CS2-*Math1*; 33); *b) Gli1*, by SP6 polymerase from mouse *Gli1* cDNA (of which we cloned a 392 nt long region of exon 13 into HindIII5′-EcoRI3′ sites of pcDNA3 vector); *c) Patched1*, by SP6 polymerase from mouse *Patched1* cDNA (of which we cloned a 515 nt long region of exon 23 into HindIII5′-EcoRI3′ sites of pcDNA3 vector); *d)* endogenous *PC3* (*i.e.*, *Tis21*), by T3 polymerase from the construct pT7T3D-*Tis21* (mouse cDNA Image 836540). No signal was detected using the corresponding sense probes.

RNA extraction, real-time RT-PCR

Total cellular RNA, obtained from tissues and cell lines according to the procedure of Chomczynski and Sacchi (34), was reverse-transcribed as described previously (25).

Total RNA from murine and human medulloblastomas (snap-frozen in liquid nitrogen), cerebellar granule cells, or PC12 cells was analyzed by real-time RT-PCR amplification, performed with a 7900HT System (Applied Biosystems, Foster City, CA, USA), using either TaqMan probe-based fluorogenic 5′ nuclease chemistry (for medulloblastomas) or SYBR GreenI dye chemistry (for cells), in duplicate samples. Relative quantification was performed by the comparative cycle-threshold method (35). Control human adult cerebellar RNA was from Clontech (Cambridge, UK) and fetal cerebellar RNA from Biocat (Heidelberg, Germany). The expression values of PC3 in human medulloblastomas were normalized to three different endogenous controls: β*Actin*, *GAPDH*, *hypoxanthine phosphoribosyltransferase*. Endogenous controls used for murine medulloblastomas were β*Actin*, β*2-microglobulin*, *hypoxanthine phosphoribosyltransferase*, whereas for cerebellar granule cells and PC12 cells TATA-binding protein and/or *18S* RNAs were used.

Specific real-time RT-PCR primers for mRNAs of *BTG2* (human *PC3*), *Tis21* (mouse *PC3*), *PC3*, and rat *cyclin D1* and of the endogenous controls were deduced from published murine cDNA sequences and are available on request.

Cell culture and infection by adenoviruses

PC12 cells were grown in Dulbecco's modified Eagle's medium with 5% supplemented calf serum and 5% horse serum (HyClone, Logan, UT, USA) in a humidified atmosphere of 12% CO_2 at 37°C. Cerebellar granule cultures from Wistar 7-day-old (P7) rats were prepared as described previously (28).

The generation of recombinant adenovirus expressing *PC3* (Adeno-*PC3*) was described previously (28). β-galactosidase

adenovirus was kindly provided by M. Crescenzi. HEK293 cells were used to propagate adenoviruses and to measure the viral titers by plaque formation assays; these were always in the range of 10^8–10^9 plaque-forming units (pfu)/ml.

Chromatin immunoprecipitation (ChIP)

Primary cultures of cerebellar granule cells infected with adeno-*PC3* or adeno-β-galactosidase or cultures of PC12 cells induced to differentiate by NGF were fixed with 1% formaldehyde. Then, chromatin was prepared from cell lysates in SDS lysis buffer (1% SDS, 10 mM EDTA, 50 mM Tris-HCl pH 8) according to standard protocols (Upstate Biotechnology), as described (36). Cellular lysates were sonicated to obtain DNA fragments of average size of 500 bp, immunoprecipitated with anti-*PC3* A3H or antiacetyl-histone-H4 antibodies, or preimmune serum as control. The presence of the rat *cyclin D1* promoter was analyzed by PCR using primers amplifying a region 770 nt before the transcription start: 5′-CCCCAGCGAG-GAGGAATAGATG-3′, 5′-TGCCAGACGAGCCCTAAGTTC-3′.

Glutathione-S-transferase (GST) fusion proteins

Pull-down assays were performed incubating 10 μl of GST proteins bound to glutathione-Sepharose resin beads with *in vitro*-programmed nuclease-treated rabbit reticulocyte lysates, as described (37). HDAC1 and HDAC4 were transcribed *in vitro* using the constructs pSCT-HDAC1, generated by subcloning in 5′*Bam*HI-3′ *Xba*I of the pSCT1 vector the coding region of HDAC1 (excised from pcDNA3.HDAC1-Flag obtained from T. Kouzarides, Cambridge, UK), and pcDNA3.1-Myc-HDAC4, provided by T. Kouzarides.

RESULTS

PC3 has tumor suppressor activity in medulloblastoma

To test the hypothesis that the *PC3* gene may suppress tumorigenesis in cerebellar GCPs, we crossed *Patched1* heterozygous mice, prone to develop spontaneous medulloblastoma, with bitransgenic mice conditionally expressing *PC3* under control of the tet-off system (Tg βACT-tTA/TRE-*PC3*, named hereafter Tg*PC3*) (28). In Tg*PC3* mice the expression of transgenic *PC3*, regulated by the β-actin (βACT) promoter, matches the expression of endogenous *PC3* in neuronal precursors undergoing neurogenic division, including GCPs (28).

To target the effect of *PC3* to neuronal precursors proliferating perinatally, *i.e.*, essentially cerebellar GCPs, whose largest wave of maturation occurs from birth to P7, the *PC3* transgene was expressed after E18—by withdrawal of doxycycline. Moreover, all the progeny of breedings between *Patched1* heterozygous and Tg*PC3* mice was irradiated at P1, a treatment increasing the frequency of medulloblastomas (22).

The F1 progeny of crosses between *Patched1* heterozygous and Tg*PC3* mice (hereafter referred to as $Ptc^{+/-}$/Tg*PC3* and $Ptc^{+/+}$/Tg*PC3* if both the βACT-tTA and the TRE-*PC3* transgenes were inherited, or $Ptc^{+/-}$ and $Ptc^{+/+}$ if they were not) did not show early lethality due to irradiation. A high incidence of medulloblastoma was observed in $Ptc^{+/-}$ mice. Of the 64 mice in this

group 39 (60.9%) developed medulloblastoma between 12 and 40 wk of age. In contrast, $Ptc^{+/-}/TgPC3$ showed a highly decreased frequency (37.5%; 9/24 total) with no significant changes in tumor latency (**Fig. 1** and **Table 1**). Therefore, $PC3$ appears to possess a strong tumor suppressive activity *in vivo*. No medulloblastoma developed after irradiation in $Ptc^{+/+}/TgPC3$ (0/30 total) or in $Ptc^{+/+}$ mice (0/67 total) (Table 1).

$PC3$ counteracts the activity of Shh in GCPs by reducing proliferation and enhancing differentiation

To gather information on the mechanisms underlying the tumor suppression by $PC3$, we sought to analyze the response of GCPs to the actions exerted by the *Shh* pathway and by $PC3$, during the initial phases of medulloblastoma tumorigenesis.

It has been previously shown that *Patched1* heterozygous mice present thicker EGL regions containing highly proliferating GCPs, defined by Kim *et al.* (20) hyperplastic EGL remnants or rests, that persist after P14. Since their incidence is higher than the frequency of medulloblastoma, these hyperplastic EGLs can be considered non committed premalignant lesions. Thus, we decided to analyze the EGL of cerebella at P14, because at this stage hyperplastic EGL regions and other pretumoral abnormalities are already detectable in *Patched1* heterozygous mice and coexist with the normal EGL, reduced to a thickness of few layers of GCPs (38, 20).

The incidence of hyperplastic EGL areas, bromodeoxyuridine (BrdU) incorporation, and expression of *cyclin D1*, *cyclin D2*, and *cyclin B1* were examined in the
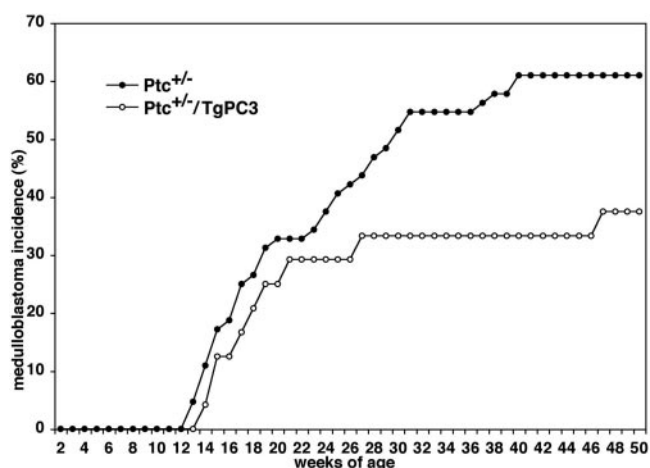

Figure 1. Suppression of medulloblastoma growth in *Patched1* heterozygous mice expressing $PC3$. The F1 progeny of crossings between mice lacking one *Patched1* allele and the Tg βACT-tTA/TRE-$PC3$ (Tg$PC3$), conditionally overexpressing $PC3$ after E18, was irradiated at P1 (3 Gy) and monitored throughout the whole life span for the onset of medulloblastoma. Medulloblastoma incidence was significantly reduced in $Ptc^{+/-}/TgPC3$ mice, expressing PC3 in GCPs (37.5%) compared with $Ptc^{+/-}$ mice lacking the $PC3$ transgene (60.9%); $P < 0.05$ (χ^2 test; see also Table 1).

cerebellum of $Ptc^{+/-}$ and $Ptc^{+/+}$ F1 mice lacking the $PC3$ transgene. At P14, cerebella of $Ptc^{+/-}$ mice presented localized, thick hyperplastic EGL regions containing up to 15–20 layers of highly proliferating GCPs (shown in **Fig. 2**A, B), with average frequency of 2.75 ± 0.48 per cerebellum (**Table 2**). Throughout the entire EGL length, but particularly in these hyperplastic regions, the frequency of GCPs incorporating BrdU or expressing *cyclin D1* resulted highly increased as compared with $Ptc^{+/+}$ wild-type mice (Fig. 2B; **Table 3**). In contrast, the expression of other cyclins, *i.e.*, *cyclin D2* and *cyclin B1*—controlling G1 and G2/M phases, respectively—was not significantly changed in the EGL of $Ptc^{+/-}$ mice compared with wild-type $Ptc^{+/+}$ mice (Table 3).

A most prominent effect of $PC3$ overexpression was a drastic reduction, up to four-fold, of the frequency of hyperplastic EGL regions in $Ptc^{+/-}/TgPC3$ mice, compared with $Ptc^{+/-}$ mice (Table 2). Concomitantly, the proliferation of GCPs throughout the EGL and hyperplastic areas, as measured by BrdU incorporation and *cyclin D1* expression, was restored to the level of wild-type $Ptc^{+/+}$ mice (Fig. 2B; Table 3). Overall, these data indicate that perinatal up-regulation of $PC3$ expression may effectively counteract the hyperproliferative stimulus caused by deregulation of the *Shh* pathway in GCPs.

Next, we examined the expression of neurogenic markers. As shown in Fig. 2B and Table 3, a strong decrease of the expression of *NeuN*, which marks post-mitotic differentiated granule neurons (39), was observed in the hyperplastic EGL regions and also in the internal granular layer (IGL) of $Ptc^{+/-}$ mice, as compared with wild-type $Ptc^{+/+}$ mice. The reduced expression of *NeuN* in the IGL, where postmitotic granule cells migrate, suggests a reduced production of differentiated granule cells by the active GCP pool in the EGL. In $Ptc^{+/-}$ mice we also detected a significant increase of the neurogenic transcription factor *NeuroD1*, within the whole hyperplastic EGL and in the IGL (Fig. 2B and Table 3) and a slight increase of the expression of *Math1* mRNA, which is required for the neurogenesis of granule neurons and is expressed in proliferating GCPs of the outer EGL (40). The increase of *NeuroD1* occurred not only in recently differentiated postmitotic GCPs of the inner EGL, as normally occurs (41), but also in proliferating undifferentiated GCPs, which may indicate a failed attempt of GCPs to differentiate.

Remarkably, in $Ptc^{+/-}/TgPC3$ mice the expression of *NeuN* was restored to the levels of wild-type $Ptc^{+/+}$ mice (Fig. 2B; Table 3). Furthermore, the EGL of $Ptc^{+/-}/TgPC3$ mice presented an evident increase in the expression of *Math1* and *NeuroD1*, compared with $Ptc^{+/-}$ mice (Fig. 2B; Table 3). In addition, the increase of *NeuroD1* positive cells was associated to a decrease of BrdU-incorporating cells (compare $Ptc^{+/-}/TgPC3$ and $Ptc^{+/-}$ EGLs in Table 3), strongly suggesting that in fact $PC3$ induced the expression of *NeuroD1* in GCPs that

TABLE 1. *Statistical analysis of medulloblastoma incidence[a]*

Genotype	$Ptc^{+/-}$	$Ptc^{+/+}$	$Ptc^{+/-}/TgPC3$	$Ptc^{+/+}/TgPC3$
Medulloblastoma (%)	39 (60.9)	0 (0.0)	9* (37.5)	0 (0.0)
Average latency (weeks)	22.31 ± 1.3	–	21.44 ± 3.4	–
Number of mice	64	67	24	30

[a] The four genotypes refer to the progeny of breedings between Patched1 heterozygotes and Tg*PC3* mice; $Ptc^{+/-}$ and $Ptc^{+/+}$ mice are in Tg background but lack βACT-tTA and TRE-*PC3* transgenes. * $P < 0.05$ *vs.* $Ptc^{+/-}$ group (Chi square test).

have ceased proliferating and become postmitotic. Such possibility is also supported by *NeuroD1*/BrdU double-staining analyses (data not shown).

Taken together, the above data indicate that the *PC3* gene not only prevents the *Patched1*-dependent hyperproliferation of GCPs within hyperplastic EGL regions, but also restores their ability to terminally differentiate.

As a further analysis of possible mechanisms of tumor suppression by *PC3*, we tested whether apoptosis of GCPs was involved. No significant change in the number of cells undergoing apoptosis in the EGL of $Ptc^{+/-}$/ Tg*PC3* vs. $Ptc^{+/-}$ mice was observed (Table 3).

Moreover, lack of difference in acute cellular response to DNA damage between $Ptc^{+/-}/TgPC3$ and $Ptc^{+/-}$ or $Ptc^{+/+}$ mice at P1, as evaluated by measuring the percentage of GCPs expressing phosphorylated histone H2A.X or undergoing apoptosis 3 h postirradiation, clearly indicates that the tumor suppressor action
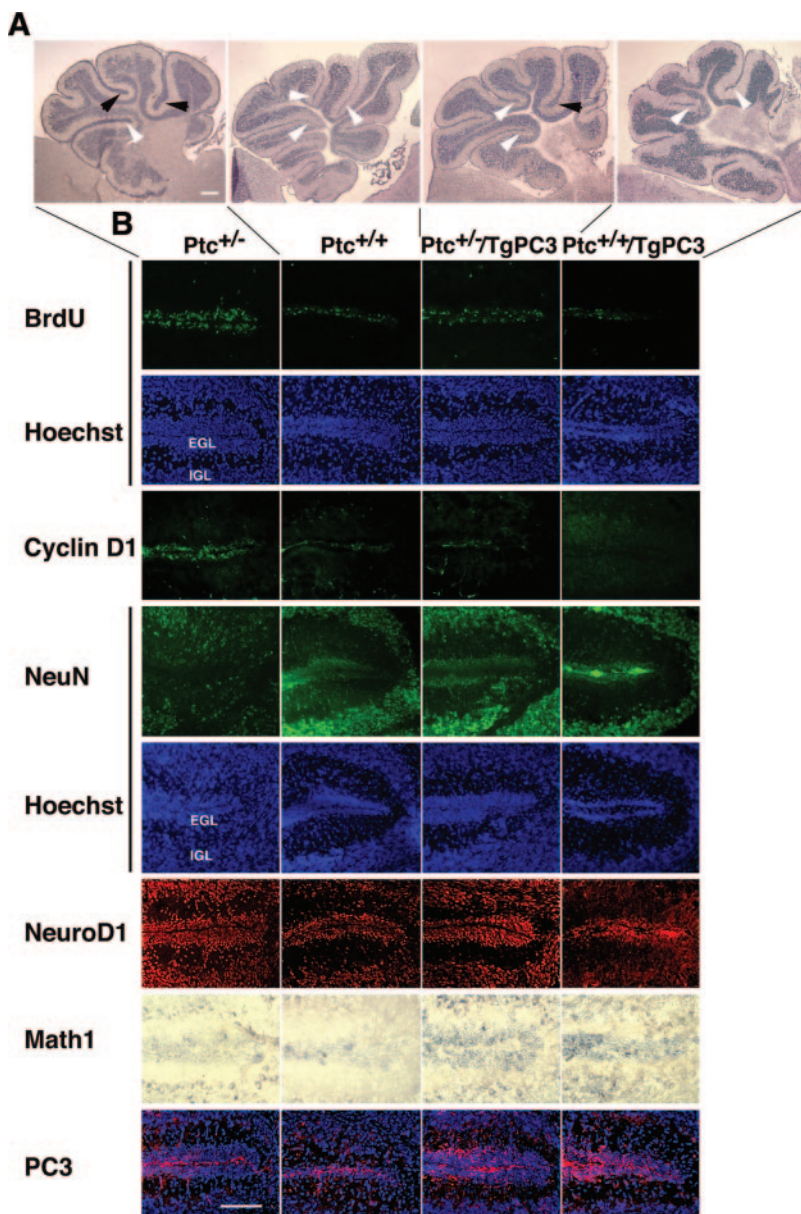

Figure 2. Increased proliferation and reduced differentiation of GCPs in hyperplastic EGL regions of $Ptc^{+/-}$ mice are reversed by PC3. *A)* Representative hyperplastic and normal EGL regions (indicated by black or white arrow heads, respectively), detected by hematoxylin staining in cerebella of $Ptc^{+/-}$, $Ptc^{+/+}$, $Ptc^{+/-}$/ Tg*PC3*, and $Ptc^{+/+}$/Tg*PC3* mice at P14. Scale bar, 235 μm. *B)* Representative sections of hyperplastic EGL regions at P14 from $Ptc^{+/-}$ and $Ptc^{+/-}$/Tg*PC3* mice, and of normal EGLs from control $Ptc^{+/+}$ and $Ptc^{+/+}$/Tg*PC3* mice, labeled with antibodies against BrdU, *cyclin D1*, *NeuN*, *NeuroD1*, *PC3*, as indicated. *Math1* mRNA was detected by in situ hybridization using specific digoxigenin-labeled probes visualized by alkaline phosphatase-conjugated secondary antibodies. The nuclear staining by Hoechst 33258 is shown for sections labeled by anti-BrdU, anti-*NeuN*, and anti-*PC3* antibodies and can be considered representative for the other sections; PC3 (red) and Hoechst staining were overlaid. An increase of proliferation, detectable as higher BrdU incorporation and expression of *cyclin D1*, and an impairment of terminal differentiation—indicated by reduced expression of *NeuN*—is evident in the EGL of $Ptc^{+/-}$ mice compared with control $Ptc^{+/+}$ mice. Paradoxically, *NeuroD1* expression is increased in $Ptc^{+/-}$ cerebella. In hyperplastic EGL regions of $Ptc^{+/-}$/Tg*PC3* mice, overexpressing *PC3* in GCPs, proliferation, and differentiation are restored to normal values, as judged by BrdU, *cyclin D1*, and *NeuN* expression. The anti-*PC3* antibody labels both endogenous and exogenous *PC3*. EGL sagittal sections were spaced 20 μm and localized in the area between lobules III and IV. Scale bar, 100 μm.

TABLE 2. *Reduced incidence of hyperplastic EGLs and lesions in $Ptc^{+/-}$ mice expressing PC3 ($Ptc^{+/-}$/TgPC3)[a]*

Genotype	$Ptc^{+/-}$	$Ptc^{+/+}$	$Ptc^{+/-}$/TgPC3	$Ptc^{+/+}$/TgPC3
Hyperplastic EGL (number/cerebellum)	2.75 ± 0.48*	0.0 ± 0.00	0.67 ± 0.33	0.0 ± 0.00
Lesions (number/cerebellum)	2.0 ± 0.41*	0.0 ± 0.00	0.33 ± 0.33	0.0 ± 0.00
Mice analyzed	4	3	3	4

[a] The parameters reported were measured in each mice by analyzing the whole cerebellum through sagittal sections spaced approximately 300 μm. * $P < 0.03$ *vs.* $Ptc^{+/-}$/TgPC3 group (Student's *t* test.).

of PC3 does not involve protection from DNA damage ($Ptc^{+/-}$/TgPC3: 13.8±1.1% phospho-H2A.X-positive GCPs and 9.1±1.0% TUNEL-positive GCPs; $Ptc^{+/-}$: 14.5±0.8% and 8.2±1.4%, respectively; $Ptc^{+/+}$: 12.7±1.2% and 11.0±1.4%, respectively. Fourteen sections analyzed per group).

The expression of endogenous *PC3* is down-regulated in preneoplastic lesions

In addition to hyperplastic EGL areas, $Ptc^{+/-}$ mice presented cerebellar lesions, consisting in EGLs abnormally expanded as nodular formations inside the cerebellar lobules. These early lesions were formed by GCPs with an even higher rate of BrdU incorporation and *cyclin D1* expression, and with lower differentiation capacity, as indicated by the greatly reduced expression of *NeuN* (see a representative image in **Fig. 3A, B**; Table 2 and 3). These formations also showed reduced expression of *Patched1* (Fig. 3B) and, having lost the organization in layers typical of the EGL, represented preneoplastic lesions at a more advanced stage than hyperplastic EGLs. As shown in Table 2, the frequency of such lesions in cerebella of $Ptc^{+/-}$/TgPC3 mice resulted 6-fold lower than in $Ptc^{+/-}$ mice.

We have previously observed that the physiological expression of *PC3* occurs mainly in the outer EGL, in the pool of proliferating GCPs, and that overexpression of *PC3* stimulates these GCPs to generate differentiated granule cells, through induction of a neurogenic division (28). Remarkably, in $Ptc^{+/-}$ cerebella we found

that endogenous *PC3* was significantly expressed only in the superficial layers of the lesions, then decreased internally and was totally absent in deeper regions, where GCPs still continued to actively proliferate and to express *cyclin D1* (compare Fig. 3B with C). *Math1* and *NeuroD1* were expressed with a distribution similar to *PC3*, whereas *Gli1*—a direct downstream target of *Shh*—was up-regulated in the deeper part of the lesion. Thus, GCPs of the internal part of the lesion showed the highest activation of the *Shh* pathway and a concomitant down-regulation of *PC3*, which strongly suggests that the decrease of endogenous *PC3* correlates with the severity of the lesion.

PC3 mRNA is down-regulated in medulloblastoma

In view of the above data, we sought to measure the endogenous levels of *PC3* mRNA in medulloblastomas from $Ptc^{+/-}$ mice. We screened a panel of 15 medulloblastomas developed in $Ptc^{+/-}$ mice of different backgrounds (*i.e.*, the mixed CD1/BDF1 background of $Ptc^{+/-}$ mice crossed with TgPC3 or the CD1 background of parental *Patched1* heterozygous mice). Cerebella from wild-type P5 mice of the corresponding background were used as appropriate control (15). As shown in **Fig. 4A**, ~50% of tumors (7 out of 15) from $Ptc^{+/-}$ mice displayed reduced expression of endogenous *PC3* mRNA, irrespective of the genetic background.

Next, we examined the expression of *PC3* in human medulloblastomas of different histotypes (Fig. 4B).

TABLE 3. *Increased proliferation and reduced differentiation of GCPs in the EGL of $Ptc^{+/-}$ mice are reversed by PC3[a]*

Genotype	EGL (%positive/total cells)				Lesions
	$Ptc^{+/-}$	$Ptc^{+/+}$	$Ptc^{+/-}$/TgPC3	$Ptc^{+/+}$/TgPC3	$Ptc^{+/-}$
BrdU	46.6 ± 1.76**	36.3 ± 1.40	32.2 ± 0.67	28.7 ± 1.54^	61.6 ± 1.76*
Cyclin D1	20.4 ± 1.29**	11.5 ± 1.17	11.4 ± 0.64	8.4 ± 1.02^	35.5 ± 3.35*
Cyclin D2	23.9 ± 1.22	23.3 ± 1.59	26.1 ± 0.87	23.0 ± 1.58	33.1 ± 2.97*
Cyclin B1	5.9 ± 0.42	6.6 ± 0.37	6.2 ± 0.68	6.6 ± 0.68	7.8 ± 0.49
NeuN	38.0 ± 1.83**	53.8 ± 2.10	53.9 ± 1.52	59.7 ± 3.14	23.1 ± 6.28*
NeuroD1	74.2 ± 1.84†	58.5 ± 0.96	86.2 ± 1.60†	74.3 ± 2.78†	52.1 ± 8.08*
TUNEL	6.8 ± 0.63	7.4 ± 0.82	5.5 ± 0.80	6.5 ± 0.96	5.3 ± 0.36

[a] For each genotype indicated, the entire EGL of three cerebella from P14 mice was analyzed (at least five sagittal sections per cerebellum, spaced ~300 μm). Sections were double-labeled with Hoechst 33258 and with BrdU, *cyclin D1, cyclin D2, cyclin B1, NeuN,* or *NeuroD1* antibodies (followed by FITC- or TRITC-conjugated secondary antibodies) or with TUNEL assay. Positive cells were identified by merging the two digital images. Values are expressed as percent ratio between cells in the EGL or in lesions positive for BrdU, *cyclin D1, cyclin D2, cyclin B1 NeuN, NeuroD1* or TUNEL and the total number of cells present. **$P < 0.001$ *vs.* $Ptc^{+/-}$/TgPC3, $Ptc^{+/+}$ or $Ptc^{+/+}$/TgPC3; ^$P < 0.01$ *vs.* $Ptc^{+/-}$/TgPC3; *$P < 0.01$ *vs.* $Ptc^{+/-}$; † $P < 0.001$ *vs.* $Ptc^{+/+}$; Student's *t* test.
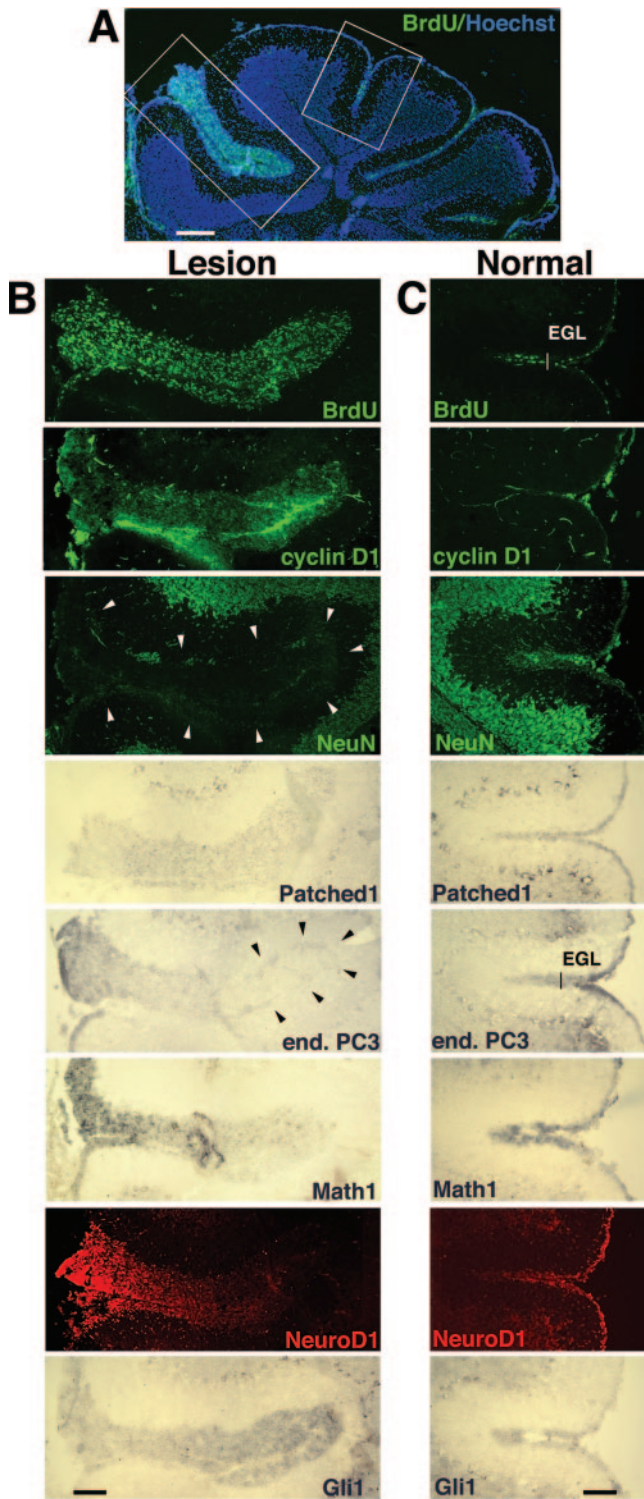
Figure 4. Down-regulation of endogenous *PC3* mRNA in murine and human medulloblastoma. *A)* Medulloblastomas 1–15 were from *Ptc*$^{+/-}$ mice of different backgrounds: *i.e.*, the mixed CD1/BDF1 background of *Ptc*$^{+/-}$ mice crossed with Tg*PC3* (1–7) or the CD1 background of parental *Ptc*$^{+/-}$ mice (8–15). Control RNA of murine medulloblastomas was from cerebella of P5 wild type mice (*n*=2) of the corresponding genetic background. *B)* Human medulloblastomas are grouped according to histotype classification. Control of human medulloblastomas was from adult cerebella. In (*A, B*) *PC3* mRNA levels were measured by quantitative real-time PCR, using primers amplifying within the coding region of murine or human mRNAs. *PC3* mRNA levels are represented as fold-expression values relative to the level of control samples, which was set to unit. Fold-expression values were log transformed, thus the level of control samples corresponds to 0 on the *y*-axis.

Figure 3. Down-regulation of endogenous *PC3* in neoplastic cerebellar lesions of *Ptc*$^{+/-}$ mice. *A)* A cerebellar sagittal section from a P14 *Ptc*$^{+/-}$ mouse, double-stained by Hoechst 33258 and BrdU. A representative lesion and normal EGL are delimited by a rectangle on the left and on the right, respectively. Scale bar, 200 μm. *B, C)* Analysis by ISH and immunohistochemistry of the cerebellar lesion (*B*) and of the normal EGL (*C*), corresponding to regions delimited by rectangles in (*A*). *B)* GCPs in the lesion show high incorporation of BrdU and expression of *cyclin D1*; in the internal part of the lesion (black arrowheads) GCPs fail to express endogenous *PC3*
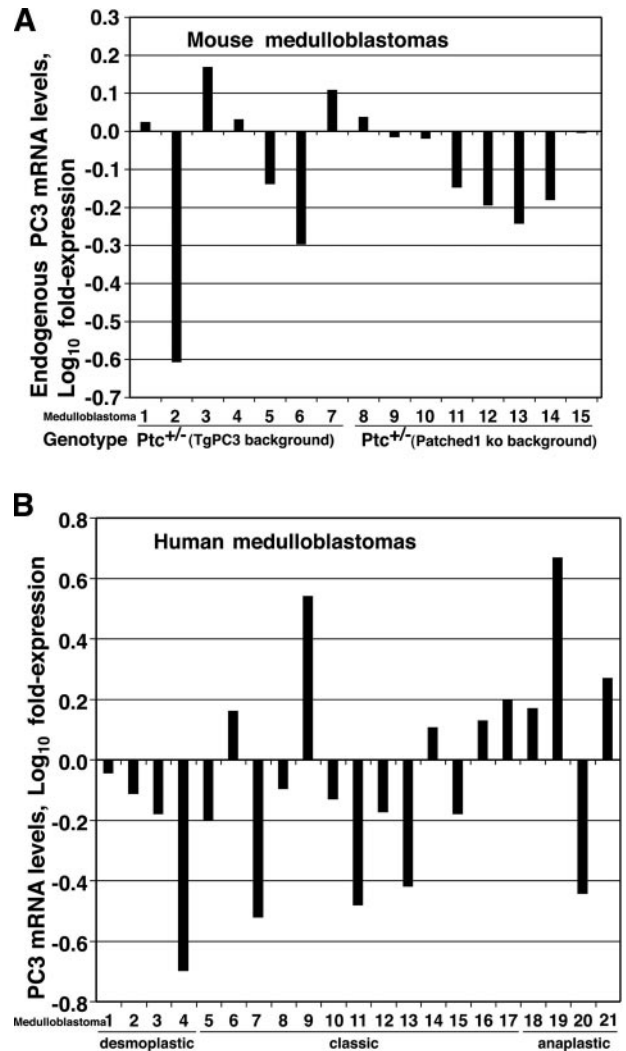
(end. *PC3*), *NeuroD1*, and *Math1*, while *Gli1* is up-regulated. *Patched1* is expressed very weakly in the lesion compared to the control EGL—see the corresponding panel (*C*). Expression of *NeuN* is barely detectable in the whole lesion area (white arrowheads). Endogenous *PC3*, *Math1*, *Gli1*, and *Patched1* were detected by specific *in vitro* transcribed antisense digoxigenin labeled probes. Adjacent sagittal sections were spaced 10 μm. Scale bars in (*B, C*), 100 μm.

Endogenous *PC3* was decreased in all human medulloblastomas of the desmoplastic histotype analyzed (*n*=4), in 8 out of 13 of the classic subtype and in 1 out of 4 of the anaplastic subtype. A pool of cerebellar RNAs from adult male and female Caucasians was used as control. Expression of PC3 in this pool resulted nearly identical to levels measured in fetal human cerebella (data not shown).

Thus, *PC3* mRNA is down-regulated in mouse and human medulloblastomas, consistently with the reduced expression of *PC3* observed in preneoplastic lesions of $Ptc^{+/-}$ cerebella.

### *PC3* interacts with the *cyclin D1* promoter region

The above data point to a central role of *cyclin D1* in the *PC3*-mediated inhibition of proliferation of normal and preneoplastic GCPs *in vivo*, as *cyclin D1*, among the tested cyclins, is selectively down-regulated by *PC3* (see Table 3). Thus, we sought to define whether *PC3* transcriptionally controls *cyclin D1* in GCPs and, more importantly, whether this control is direct. Therefore, we determined *cyclin D1* mRNA levels in primary cultures of granule cells infected with *PC3*-expressing adenovirus, as well as in the neuronal PC12 cell line treated with nerve growth factor (NGF), a stimulus known to highly induce *PC3* expression (23). As shown in **Fig. 5A, B**, the expression of ectopic *PC3* in cerebellar granule cells, or the induction of endogenous *PC3* in PC12 cells, was accompanied by a corresponding decrease of the levels of *cyclin D1* mRNA.

Next, we asked whether *PC3* is recruited to the *cyclin D1* promoter. To this aim, we performed chromatin immunoprecipitation (ChIP) experiments on primary cultures of granule cells and in PC12 cells, treated as above, using the anti-*PC3* antibody A3H (24). Amplification by PCR of a fragment of the *cyclin D1* promoter region showed that *PC3* resided on the *cyclin D1* promoter both in cerebellar granule and PC12 cells and that the levels of *PC3* bound to the promoter were higher in cerebellar granule cells infected with *PC3*-expressing adenovirus and in PC12 cells after induction of endogenous *PC3* by NGF (Fig. 5*C, D*). Furthermore, the increased binding of *PC3* to the *cyclin D1* promoter was accompanied by decreased levels of acetylated histone H4 associated to the promoter (Fig. 5*C, D*, panel anti-acetyl-H4), suggesting that *PC3* binding may inhibit *cyclin D1* transcription by promoting histone deacetylation at the *cyclin D1* promoter. An implication of this hypothesis is that *PC3* might recruit histone deacetylases (HDACs) to the *cyclin D1* promoter. To test this possibility, we performed a GST pull-down assay to analyze the ability of *PC3* to bind HDAC1 and HDAC4. Both *in vitro*-translated histone deacetylases resulted specifically able to associate with GST-*PC3* (Fig. 5*E*).

As a whole, these data strongly suggest that *PC3*

Figure 5. *PC3* binds the *cyclin D1* promoter and inhibits *cyclin D1* transcription by decreasing histone H4 acetylation, possibly through recruitment of HDAC1 and HDAC4. *A, B)* Real-time RT-PCR analysis of *PC3* and *cyclin D1* mRNA in cerebellar granule cells and in PC12 cells. Cerebellar granule cells, obtained from P7 rats, were plated and infected with recombinant adenoviruses adeno-*PC3* or control adeno-β-galactosidase either the day of plating (DIV 0) or after 4 d (DIV 4), and harvested after 48 h (at DIV 2 or DIV 6, respectively). PC12 cells were treated with NGF (100 ng/ml) for the indicated times. The primers amplifying *PC3* detected both the endogenous and exogenous mRNA. Average ± SEM values are from three replicates. TATA-binding protein mRNA was used as endogenous control for normalization. *C, D)* Representative ChIP assays (from a total of three experiments) in primary cultures of cerebellar granule cells and in PC12 cells, infected or treated with NGF as indicated in (*A, B*), using either anti-*PC3* A3H or antiacetyl-histone-H4 antibodies, or preimmune serum. Input: PCR performed using *cyclin D1* promoter primers on the cell lysates used for ChIP. The up-regulation of *PC3* mRNA, elicited either by adeno-*PC3* or by NGF, matches the increases of *PC3* associated to *cyclin D1* promoter, while it appears inversely correlated with histone H4 acetylation. *E)* *PC3* interacts *in vitro* with HDAC1 and HDAC4. ^{35}S-labeled HDAC1 and HDAC4 *in vitro*-translated in rabbit reticulocyte lysates were incubated with GST-*PC3* or GST-fused proteins bound to glutathione-Sepharose 4B. Bound proteins were eluted and analyzed by SDS–8% PAGE, followed by autoradiography. The labeled input products loaded were ~10% of the amount used in the pull-down incubations.
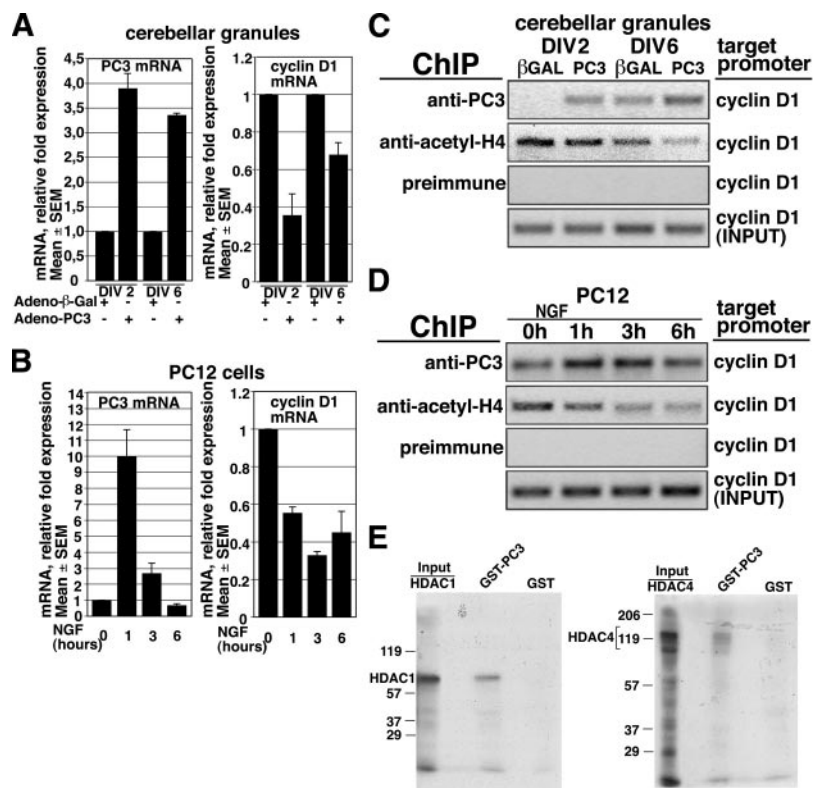
negatively controls the transcription of *cyclin D1* by directly associating to the promoter, possibly recruiting to it HDAC1 and HDAC4.

DISCUSSION

This report provides the first evidence that *PC3* acts as tumor suppressor in the central nervous system. In fact, we observed a drastic reduction of medulloblastoma incidence, following *PC3* up-regulation in preneoplastic cerebellar GCPs of the *Patched1* heterozygous mouse model.

Important issues raised by these observations concern the molecular mechanism by which the *PC3*-mediated tumor suppression occurs, and the possible role of endogenous *PC3* down-regulation in the process of medulloblastoma tumorigenesis.

PC3 restores to normality the proliferation of GCPs in *Ptc*$^{+/-}$ mice

The capability to undergo massive expansion during postnatal development before terminal differentiation is a peculiar feature of GCPs of the EGL. Thus, a tight control of the transition from a mitotically active, undifferentiated state to postmitotic terminal differentiation is critical for these neural precursor cells. *Cyclin D1*, *cyclin D2*, and *N-Myc* are essential for cerebellar organogenesis (42, 9) and lead to GCP proliferation in response to *Shh* signaling (6, 8). Accordingly, persistent expression of such genes is recurrent in childhood medulloblastomas.

Our analysis of cerebella of *Ptc*$^{+/-}$ mice at P14 evidenced several abnormalities preceding medulloblastoma appearance. In first place, localized hyperplastic EGL regions, where GCPs showed an increased rate of proliferation, as measured by BrdU incorporation and *cyclin D1* expression. More advanced alterations consisted in focal lesions, in which GCPs displayed a further increase in BrdU incorporation and very high expression of downstream targets of the *Shh*/*Patched1* pathway, *i.e.*, *cyclin D1* and *Gli1* (6, 8, 43). Thus, the hyperproliferating EGL regions and the focal lesions observed at P14 appear preneoplastic formations at different levels of commitment, triggered by a strong proliferative stimulus originating from deregulated *Shh* pathway activation.

A most evident effect of *PC3* overexpression in *Ptc*$^{+/-}$ cerebella was the reversal of *Shh*-dependent hyperproliferation, throughout the entire EGL and particularly in the hyperplastic regions. This effect is linked to the ability of *PC3* to delay cell cycle progression from G1 to S phase, as indicated by the reduced incorporation of BrdU in the EGL of *Ptc*$^{+/-}$/Tg*PC3* mice at P14. We show that this delay occurs through specific down-regulation by *PC3* of the levels of *cyclin D1* - well known to trigger with the partner cyclin-dependent kinase 4/6 the entry into S phase—as no significant change was observed in the expression of other cyclins.

Down-regulation of *cyclin D1* levels suggests that a specific interaction of PC3 with *cyclin D1* is involved in the mechanism of tumor suppression. In this regard, results from previous studies have shown no interference of *PC3* with *N-Myc* (28), a direct target of *Shh* responsible for the up-regulation of *cyclin D1* in GCPs (7, 10).

Indeed, as the present chromatin immunoprecipitation studies in GCPs reveal, *PC3* is recruited to the *cyclin D1* promoter, in correlation with reduced histone acetylation at the promoter. We also observed that *PC3* can directly interact with HDAC1 and HDAC4. Taken together, these observations strongly suggest that *PC3* negatively controls *cyclin D1* transcription by participating to deacetylase-containing repressor complexes on the *cyclin D1* promoter.

Therefore, the functional antagonism to *Shh* exerted by *PC3* in GCPs occurs through direct inhibition of the Shh downstream target *cyclin D1*. In line with our results, *cyclin D1*$^{-/-}$/*Ptc*$^{+/-}$ double knockout mice develop medulloblastomas with significantly lower incidence than *Ptc*$^{+/-}$ mice (44).

Growth arrest by *PC3* is associated to a neurogenic effect in preneoplastic GCPs

Another prominent feature of hyperplastic EGLs and preneoplastic lesions of *Ptc*$^{+/-}$ mice was the presence of marked differentiation defects, as indicated by reduced expression of *NeuN* and also by a paradoxical increase of *NeuroD1* (*i.e.*, not restricted to the postmitotic GCPs where it is normally expressed). A similar inhibition of differentiation has also been previously observed in cultures of GCPs kept under the proliferative stimulus of *Shh* (3).

Notably, *PC3* overexpression rescued GCPs differentiation, as indicated by restoration of normal expression levels of the terminal differentiation marker *NeuN* in *Ptc*$^{+/-}$/Tg*PC3* mice. Furthermore, our results show a detectable increase in the expression of *Math1* and *NeuroD1* in the EGL of *Ptc*$^{+/-}$/Tg*PC3* mice at P14 and also suggest that *PC3* rescues at least in part the mis-expression of *NeuroD1* in proliferating GCPs of *Ptc*$^{+/-}$ mice, reestablishing its postmitotic expression. Consistent with our previous data showing that *PC3* induces transcription of *Math1* in GCPs (28) and with the observation that *Math1* induces *NeuroD1* (41), the prodifferentiative effects of *PC3* might result not only from its ability to delay G1-S progression in GCPs but also from a direct effect on proneural gene(s). *PC3*, whose expression is known to be associated with the induction of an asymmetric neurogenic division [(26–28); for review, see (45)], may, therefore, have the ability to restore the neurogenic state in *Shh*-stimulated GCPs.

Altogether, the combined abilities of *PC3* to inhibit the *Shh*-dependent hyperproliferation of GCPs and to rescue their terminal differentiation can fully account for the tumor suppressive effect of *PC3*.

Possible physiological role of *PC3* as tumor suppressor

While current knowledge indicates *PC3* as a regulator of neural progenitor development, we have identified a tumor suppressor role for *PC3* in the cerebellum. In support of this view is the observation that endogenous *PC3* was down-regulated in preneoplastic lesions of $Ptc^{+/-}$ cerebella at P14, as well as in murine and human medulloblastomas. Moreover, our experiments in the *Patched1*-deficient mouse model of medulloblastoma demonstrated tumor suppression following up-regulation of *PC3 in vivo* in proliferating GCPs, where it is normally expressed. Altogether, this suggests that *PC3* may behave physiologically as tumor suppressor.

Although our results indicate that *PC3* plays a key role in preventing medulloblastoma development from early stage, the recently generated *PC3*-null mice did not show overt alterations in the cerebellum (46). Analysis, however, was limited to the gross cerebellar morphology. Similarly, *PC3*-null mice have not been reported to develop spontaneous tumors in the early stages of their lives. A possibility is that in *PC3*-null mice the function of *PC3* is vicariated by other genes of the family to which *PC3* belongs, such as *BTG1*, *TOB*, or *PC3B* (47, 48). A second possibility, indicated by the finding that the functional ablation of *PC3* by RNA interference predisposes to tumorigenesis by allowing *Ras*-dependent cellular transformation (49), is that the inactivation of *PC3* cooperates with other oncogenic events to induce neoplastic transformation.

In agreement with our results, additional evidence suggests that *PC3* down-regulation promotes the tumorigenic process, since decreased levels of *PC3* were observed in prostate, renal, and breast cancers (50–52).

Thus, a comprehensive hypothesis, accounting for the down-regulation of *PC3* observed in medulloblastomas and preneoplastic lesions, implies the inactivation of *PC3* as a critical step for the onset of medulloblastoma. Our results, highlighting the tumor suppressive effect of PC3 overexpression *in vivo,* qualify this gene as a functional antagonist of the *Shh* pathway in medulloblastoma pathogenesis and as a potential new target for therapy. [FJ]

REFERENCES

1. Alder, J., Cho, N., and Hatten, M. (1996) Embryonic precursor cells from the rhombic lip are specified to a cerebellar granule neuron identity. *Neuron* **17,** 389–399

2. Marino, S. (2005) Medulloblastoma: developmental mechanisms out of control. *Trends Mol. Med.* **11,** 17–22

3. Wechsler-Reya, R. J., and Scott, M. P. (1999) Control of neuronal precursor proliferation in the cerebellum by Sonic hedgehog. *Neuron* **22,** 103–114

4. Dahmane, N., and Ruiz-i-Altaba, A. (1999) Sonic hedgehog regulates the growth and patterning of the cerebellum. *Development* **126,** 3089–3100

5. Wallace, V. A. (1999) Purkinje-cell-derived Sonic hedgehog regulates granule neuron precursor cell proliferation in the developing mouse cerebellum. *Curr. Biol.* **9,** 445–448

6. Kenney, A. M., and Rowitch, D. H. (2000) Sonic hedgehog promotes G1 cyclin expression and sustained cell cycle progression in mammalian neuronal precursors. *Mol. Cell. Biol.* **20,** 9055–9067

7. Oliver, T. G., Grasfeder, L. L., Carroll, A. L., Kaiser, C., Gillingham, C. L., Lin, S. M., Wickramasinghe, R., Scott, M. P., and Wechsler-Reya, R. J. (2003) Transcriptional profiling of the Sonic hedgehog response: a critical role for N-myc in proliferation of neuronal precursors. *Proc. Natl. Acad. Sci. U. S. A.* **100,** 7331–7336

8. Zhao, Q., Kho, A., Kenney, A. M., Yuk, Di, D. I., Kohane, I., and Rowitch, D. H. (2002) Identification of genes expressed with temporal-spatial restriction to developing cerebellar neuron precursors by a functional genomic approach. *Proc. Natl. Acad. Sci. U. S. A.* **99,** 5704–5709

9. Knoepfler, P. S., Cheng, P. F., and Eisenman, R. N. (2002) N-myc is essential during neurogenesis for the rapid expansion of progenitor cell populations and the inhibition of neuronal differentiation. *Genes Dev.* **16,** 2699–2712

10. Kenney, A. M., Cole, M. D., and Rowitch, D. H. (2003) N-myc upregulation by sonic hedgehog signaling promotes proliferation in developing cerebellar granule neuron precursors. *Development* **130,** 15–28

11. Hahn, H., Wicking, C., Zaphiropoulous, P. G., Gailani, M. R., Shanley, S., Chidambaram, A., Vorechovsky, I., Holmberg, E., Unden, A. B., Gillies, S., *et al.* (1996) Mutations of the human homolog of Drosophila patched in the nevoid basal cell carcinoma syndrome. *Cell* **85,** 841–851

12. Raffel, C., Jenkins, R. B., Frederick, L., Hebrink, D., Alderete, B., Fults, D. W., and James, C. D. (1997) Sporadic medulloblastomas contain PTCH mutations. *Cancer Res.* **57,** 842–845

13. Wolter, M., Reifenberger, J., Sommer, C., Ruzicka, T., and Reifenberger, G. (1997) Mutations in the human homologue of the Drosophila segment polarity gene patched (PTCH) in sporadic basal cell carcinomas of the skin and primitive neuro-ectodermal tumors of the central nervous system. *Cancer Res.* **57,** 2581–2585

14. Pietsch, T., Waha, A., Koch, A., Kraus, J., Albrecht, S., Tonn, J., Sorensen, N., Berthold, F., Henk, B., Schmandt, N., *et al.* (1997) Medulloblastomas of the desmoplastic variant carry mutations of the human homologue of Drosophila patched. *Cancer Res.* **57,** 2085–2088

15. Lee, Y., Miller, H. L., Jensen, P., Hernan, R., Connelly, M., Wetmore, C., Zindy, F., Roussel, M. F., Curran, T., Gilbertson, R. J., *et al.* (2003) A molecular fingerprint for medulloblastoma. *Cancer Res.* **63,** 5428–5437

16. Pomeroy, S. L., Tamayo, P., Gaasenbeek, M., Sturla, L. M., Angelo, M., McLaughlin, M. E., Kim, J. Y., Goumnerova, L. C., Black, P. M., Lau, C., *et al.* (2002) Prediction of central nervous system embryonal tumour outcome based on gene expression. *Nature* **415,** 436–442

17. Goodrich, L. V., Milenkovic, L., Higgins, K. M., and Scott, M. P. (1997) Altered neural cell fates and medulloblastoma in mouse patched mutants. *Science* **277,** 1109–1113

18. Hahn, H., Wojnowski, L., Zimmer, A. M., Hall, J., Miller, G., and Zimmer, A. (1998) Rhabdomyosarcomas and radiation hypersensitivity in a mouse model of Gorlin syndrome. *Nat. Med.* **4,** 619–622

19. Wetmore, C., Eberhart, D. E., and Curran, T. (2000) The normal patched allele is expressed in medulloblastomas from mice with heterozygous germ-line mutation of patched. *Cancer Res.* **60,** 2239–2246

20. Kim, J. Y., Nelson, A. L., Algon, S. A., Graves, O., Sturla, L. M., Goumnerova, L. C., Rowitch, D. H., Segal, R. A., and Pomeroy, S. L. (2003) Medulloblastoma tumorigenesis diverges from

cerebellar granule cell differentiation in patched heterozygous mice. *Dev. Biol.* **263,** 50–66

21. Pazzaglia, S., Mancuso, M., Atkinson, M. J., Tanori, M., Rebessi, S., Majo, V. D., Covelli, V., Hahn, H., and Saran, A. (2002) High incidence of medulloblastoma following X-ray-irradiation of newborn Ptc1 heterozygous mice. *Oncogene* **21,** 7580–7584

22. Pazzaglia, S., Tanori, M., Mancuso, M. T., Rebessi, S., Leonardi, S., Di Majo, V., Covelli, V., Atkinson, M. J., Hahn, H., and Saran, A. (2006) Linking DNA damage to medulloblastoma tumorigenesis in Patched heterozygous knockout mice. *Oncogene* **25,** 1165–1173

23. Bradbury, A., Possenti, R., Shooter, E. M., and Tirone, F. (1991) Molecular cloning of PC3, a putatively secreted protein whose mRNA is induced by nerve growth factor and depolarization. *Proc. Natl. Acad. Sci. U. S. A.* **88,** 3353–3357

24. Montagnoli, A., Guardavaccaro, D., Starace, G., and Tirone, F. (1996) Overexpression of the nerve growth factor-inducible PC3 immediate early gene is associated to inhibition of cell proliferation. *Cell Growth & Differ.* **7,** 1327–1336

25. Guardavaccaro, D., Corrente, G., Covone, F., Micheli, L., D'Agnano, I., Starace, G., Caruso, M., and Tirone, F. (2000) Arrest of G1-S progression by the p53-inducible gene PC3 is Rb dependent and relies on the inhibition of cyclin D1 transcription. *Mol. Cell. Biol.* **20,** 1797–1815

26. Iacopetti, P., Barsacchi, G., Tirone, F., Maffei, L., and Cremisi, F. (1994) Developmental expression of PC3 gene is correlated with neuronal cell birthday. *Mech. Dev.* **47,** 127–137

27. Iacopetti, P., Michelini, M., Stuckmann, I., Oback, B., Aaku-Saraste, E., and Huttner, W. B. (1999) Expression of the antiproliferative gene TIS21 at the onset of neurogenesis identifies single neuroepithelial cells that switch from proliferative to neuron-generating division. *Proc. Natl. Acad. Sci. U. S. A.* **96,** 4639–4644

28. Canzoniere, D., Farioli-Vecchioli, S., Conti, F., Ciotti, M. T., Tata, A. M., Augusti-Tocco, G., Mattei, E., Lakshmana, M. K., Krizhanovsky, V., Reeves, S. A., *et al.* (2004) Dual control of neurogenesis by PC3 through cell cycle inhibition and induction of Math1. *J. Neurosci.* **24,** 3355–3369

29. Gazit, R., Krizhanovsky, V., and Ben-Arie, N. (2004) Math1 controls cerebellar granule cell differentiation by regulating multiple components of the Notch signaling pathway. *Development* **131,** 903–913

30. Gossen, M., and Bujard, H. (1992) Tight control of gene expression in mammalian cells by tetracycline-responsive promoters. *Proc. Natl. Acad. Sci. U. S. A.* **89,** 5547–5551

31. Mares, V., Lodin, Z., and Srajer, J. (1970) The cellular kinetics of the developing mouse cerebellum I. The generation cycle, growth fraction and rate of proliferation of the external granular layer. *Brain Res.* **23,** 323–342

32. Gavrieli, Y., Sherman, Y., and Ben-Sasson, S. A. (1992) Identification of programmed cell death in situ via specific labeling of nuclear DNA fragmentation. *J. Cell Biol.* **119,** 493–591

33. Farah, M. H., Olson, J. M., Sucic, H. B., Hume, R. I., Tapscott, S. J., and Turner, D. L. (2000) Generation of neurons by transient expression of neural bHLH proteins in mammalian cells. *Development* **127,** 693–702

34. Chomczynski, P., and Sacchi, N. (1987) Single-step method of RNA isolation by acid guanidinium thiocyanate-phenol-chloroform extraction. *Anal. Biochem.* **162,** 156–159

35. Livak, K. J., and Schmittgen, T. D. (2001) Analysis of relative gene expression data using real-time quantitative PCR and the 2(-Delta Delta C(T)) Method. *Methods* **25,** 402–408

36. Passeri, D., Marcucci, A., Rizzo, G., Billi, M., Panigada, M., Leonardi, L., Tirone, F., and Grignani, F. (2006) BTG2 enhances retinoic acid induced differentiation by modulating histone H4 methylation and acetylation. *Mol. Cell. Biol.* **26,** 5023–5032

37. Micheli, L., Leonardi, L., Conti, F., Buanne, P., Canu, N., Caruso, M., and Tirone, F. (2005) PC4 co-activates MyoD by relieving the HDAC4-mediated inhibition of MEF2C. *Mol. Cell. Biol.* **25,** 2242–2259

38. Fujita, S., Shimada, M., and Nakamura, T. (1966) H3-thymidine autoradiographic studies on the cell proliferation and differentiation in the external and the internal granular layers of the mouse cerebellum. *J. Comp. Neurol.* **128,** 191–208

39. Weyer, A., and Schilling, K. (2003) Developmental and cell type-specific expression of the neuronal marker NeuN in the murine cerebellum. *J. Neurosci. Res.* **73,** 400–409

40. Ben-Arie, N., Bellen, H. J., Armstrong, D. L., McCall, A. E., Gordadze, P. R., Guo, Q., Matzuk, M. M., and Zoghbi, H. Y. (1997) Math1 is essential for genesis of cerebellar granule neurons. *Nature* **390,** 169–172

41. Miyata, T., Maeda, T., and Lee, J. E. (1999) NeuroD is required for differentiation of the granule cells in the cerebellum and hippocampus. *Genes Dev.* **13,** 1647–1652

42. Ciemerych, M. A., Kenney, A. M., Sicinska, E., Kalaszczynska, I., Bronson, R. T., Rowitch, D. H., Gardner, H., and Sicinski, P. (2002) Development of mice expressing a single D-type cyclin. *Genes Dev.* **16,** 3277–3289

43. Oliver, T. G., Read, T. A., Kessler, J. D., Mehmeti, A., Wells, J. F., Huynh, T. T., Lin, S. M., and Wechsler-Reya, R. J. (2005) Loss of patched and disruption of granule cell development in a pre-neoplastic stage of medulloblastoma. *Development* **132,** 2425–2439

44. Pogoriler, J., Millen, K., Utset, M., and Du, W. (2006) Loss of cyclin D1 impairs cerebellar development and suppresses medulloblastoma formation. *Development* **133,** 3929–3937

45. Gotz, M., and Huttner, W. B. (2005) The cell biology of neurogenesis. *Nat. Rev. Mol. Cell. Biol.* **6,** 777–788

46. Park, S., Lee, Y. J., Lee, H. J., Seki, T., Hong, K. H., Park, J., Beppu, H., Lim, I. K., Yoon, J. W., Li, E., Kim, S. J., and Oh, S. P. (2004) B-cell translocation gene 2 (Btg2) regulates vertebral patterning by modulating bone morphogenetic protein/smad signaling. *Mol. Cell. Biol.* **24,** 10256–10262

47. Tirone, F. (2001) The gene PC3^TIS21/BTG2, prototype member of the PC3/BTG/TOB family, regulator in control of cell growth, differentiation, and DNA repair? *J. Cell. Physiol.* **187,** 155–165

48. Matsuda, S., Rouault, J., Magaud, J., and Berthet, C. (2001) In search of a function for the TIS21/PC3/BTG1/TOB family. *FEBS Lett.* **497,** 67–72

49. Boiko, A. D., Porteous, S., Razorenova, O. V., Krivokrysenko, V. I., Williams, B. R., and Gudkov, A. V. (2006) A systematic search for downstream mediators of tumor suppressor function of p53 reveals a major role of BTG2 in suppression of Ras-induced transformation. *Genes Dev.* **20,** 236–252

50. Ficazzola, M. A., Fraiman, M., Gitlin, J., Woo, K., Melamed, J., Rubin, M. A., and Walden, P. D. (2001) Antiproliferative B cell translocation gene 2 protein is down-regulated post-transcriptionally as an early event in prostate carcinogenesis. *Carcinogenesis* **22,** 1271–1279

51. Struckmann, K., Schraml, P., Simon, R., Elmenhorst, K., Mirlacher, M., Kononen, J., and Moch, H. (2004) Impaired expression of the cell cycle regulator BTG2 is common in clear cell renal cell carcinoma. *Cancer Res.* **64,** 1632–1638

52. Kawakubo, H., Carey, J. L., Brachtel, E., Gupta, V., Green, J. E., Walden, P. D., and Maheswaran, S. (2004) Expression of the NF-kappaB-responsive gene BTG2 is aberrantly regulated in breast cancer. *Oncogene* **23,** 8310–8319